Effect of Lattice Structure on Energetic Electron Transport in Solids Irradiated by Ultraintense Laser Pulses

P. McKenna,[1,*] A. P. L. Robinson,[2] D. Neely,[2] M. P. Desjarlais,[3] D. C. Carroll,[1] M. N. Quinn,[1] X. H. Yuan,[1]
C. M. Brenner,[1,2] M. Burza,[4] M. Coury,[1] P. Gallegos,[1,2] R. J. Gray,[1] K. L. Lancaster,[2] Y. T. Li,[5] X. X. Lin,[5]
O. Tresca,[1] and C.-G. Wahlström[4]

[1]*SUPA, Department of Physics, University of Strathclyde, Glasgow G4 0NG, United Kingdom*
[2]*Central Laser Facility, STFC Rutherford Appleton Laboratory, Oxfordshire OX11 0QX, United Kingdom*
[3]*Sandia National Laboratories, P.O. Box 5800, Albuquerque, New Mexico 87185, USA*
[4]*Department of Physics, Lund University, P.O. Box 118, S-22100 Lund, Sweden*
[5]*Beijing National Laboratory of Condensed Matter Physics, Institute of Physics, CAS, Beijing 100190, China*

The effect of lattice structure on the transport of energetic (MeV) electrons in solids irradiated by ultraintense laser pulses is investigated using various allotropes of carbon. We observe smooth electron transport in diamond, whereas beam filamentation is observed with less ordered forms of carbon. The highly ordered lattice structure of diamond is shown to result in a transient state of warm dense carbon with metalliclike conductivity, at temperatures of the order of 1–100 eV, leading to suppression of electron beam filamentation.

Improving our understanding of the physics of energetic (''fast'') electron transport in dense matter is critical for many applications in high energy density physics, including the fast ignition approach to inertial confinement fusion [1], the development of laser-driven ion sources [2], and for laboratory astrophysics. It is well established that in the interaction of an ultraintense ($> 10^{19}$ W cm^{-2}) laser pulse with a solid target, a significant fraction of the laser energy is absorbed, producing a multi-mega-ampere current of relativistic electrons, and that the propagation of these fast electrons within the target is subject to transport instabilities giving rise to filamentation of the beam. Previous studies have shown that a number of plasma instabilities can cause filamentation, including the Weibel [3,4], two-stream [5], and resistive filamentation instabilities [6]. However, the precise causal agents and the circumstances under which filamentation is suppressed are not well understood.

It is well known from solid state physics that the conductivity of a material is strongly affected by its lattice structure [7]. The propagation of a high current of fast electrons in a solid target irradiated by a high energy picosecond laser pulse requires, by charge neutrality, a ''return'' current of thermal electrons which are collisional and rapidly, on the order of picoseconds, heat a significant volume of the target to temperatures in the range 1–100 eV. This results in a nonequilibrium state of warm dense matter (WDM) in which the electrons are ''warm'' (1–100 eV) but the ions remain essentially cold and maintain temporarily the structural arrangement they possessed in the condensed matter state. The conductivity of the material in this transient nonequilibrium state is strongly affected by the retained lattice structure.

In this Letter, we demonstrate for the first time, using various allotropes of a single element, carbon, that lattice structure alone can determine whether or not fast electron beam filamentation occurs in solid targets irradiated by intense picosecond laser pulses. It is shown that the highly ordered arrangement of carbon atoms in diamond results in a transient state of warm dense carbon with metalliclike conductivity, whereas disordered allotropes of carbon under similar rapid thermal loading are poorly conducting. Thus it is demonstrated that the choice of a particular allotrope of a given element enables the material conductivity in the temperature range 1–100 eV to be tailored to produce a given fast electron transport pattern.

The experiment was performed using the Vulcan laser, delivering pulses of 1.053 μm wavelength light, with an energy of 200 J (on target) and duration equal to 1 ps, FWHM. The p-polarized pulses were focused to an 8 μm diameter FWHM spot, to a calculated peak intensity of 2×10^{20} W cm^{-2}. The main target samples were three different allotropes of carbon: (1) single-crystalline diamond, (2) vitreous carbon (disordered), and (3) pyrolytic carbon, which is similar to graphite but with some degree of covalent bonding between its graphene sheets, thus presenting an intermediate degree of atomic ordering. Aluminum and plastic (Mylar) targets were also used as reference materials due to the differences in their ordering and room temperature electrical conductivity. The target size in all cases was 5 mm × 5 mm and 500 μm thick. We diagnosed the fast electron transport pattern by recording and analyzing the spatial-intensity profile of beams of protons accelerated from the rear surface of the target by an electrostatic sheath field established there by the fast electrons [2]. Filamentation of the electron beam within

the target produces modulations in the sheath field, which are mapped into the expanding proton beam spatial-intensity distribution, as demonstrated by Fuchs *et al.* [8] and discussed later. The proton beam profile measurements were made using stacked dosimetry film, which enables measurement of the dose deposited by the proton beam at discrete energies given by the stopping range of protons within the stack. Each piece of film was optically scanned and the modulations within the proton dose were quantified.

The key finding of our experiment is that the different allotropes of carbon produce very different fast electron transport patterns. This is demonstrated in Fig. 1, which shows example proton beam spatial-intensity profiles for diamond and vitreous carbon. Figure 1(c) shows the variance in proton dose (normalized to the average dose level) for the range of targets explored. Larger variance values correspond to a more structured proton beam and therefore more filamentation of the electron beam. From left to right in Fig. 1(c), as the degree of ordering of the atoms (in the cold state) increases, the proton beam becomes more uniform, indicating less filamentation. The fast electron transport pattern in diamond is smooth and free of filamentation, and is very similar to that measured for aluminum. By contrast, heavy filamentation is observed for vitreous carbon. Pyrolytic carbon and Mylar, with intermediate degrees of atomic ordering, produce intermediate levels of beam filamentation. Repeat shots were taken on each of the carbon allotropes and the results are fully reproducible, as shown in Fig. 1(c).

These results clearly show a correlation between the degree of lattice structure and the extent of fast electron beam filamentation in targets of the same element. The findings are explained by the effect of lattice structure on electrical conductivity and the fact that the structure is

temporarily maintained during rapid thermal excitation of the material [9]. To investigate this in more detail, we modeled the electronic structure and electrical conductivity of two different allotropes of carbon: diamond [tetrahedral lattice; Fig. 2(a)] and vitreous carbon [disordered; Fig. 2(b)] as a function of temperature. The electrical conductivities were derived using quantum molecular dynamics calculations with VASP, a plane-wave density functional code [10]. The atomic configurations were sampled from the configurations in 300 K simulations for each allotrope. The electronic temperature was then varied from 1 to 20 eV in subsequent static Kubo-Greenwood conductivity calculations [11] with the sampled configurations.

Figure 2(c) shows the calculated conductivity as a function of temperature for both carbon allotropes. Diamond is strongly insulating at room temperatures due to the large gap between its valence and conductance bands. However, the electrical conductivity rises sharply with the electronic temperature as soon as the electrons are excited enough to reach above the band gap. The peak in the diamond conductivity corresponds to the onset of ionization for $2s$ electrons and an average of approximately one electron per atom thermally occupying states above the band gap. In contrast, the conductivity of vitreous carbon, which is low but finite at ambient conditions, rises only weakly with increasing electronic temperature, even when heated in the same way. In the transient WDM regime (~ 10 eV), the electrical conductivity of diamond becomes nearly 2 orders of magnitude greater than that of disordered carbon. At even higher temperatures (> 100 eV), the conductivities rise sharply for both materials.

The physical origin of the effects of ionic ordering on electrical conductivity can be understood in the following way. The form of the conductivity-temperature curve in the nonequilibrium regime is critically determined by
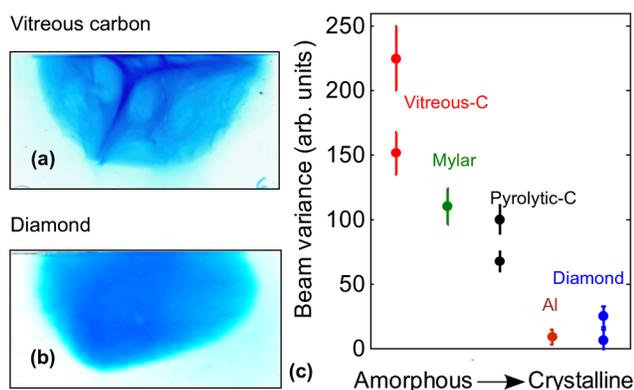

FIG. 1 (color online). Spatial-intensity profile measurements (lower half) of the proton beam, at energy 10 MeV, for (a) vitreous carbon and (b) diamond. (c) Variance in the proton signal (mean of 10 samples) near the center of the proton beam, for given target materials with increasing atomic ordering from left to right. Error bars correspond to statistical variations over the multiple samples.
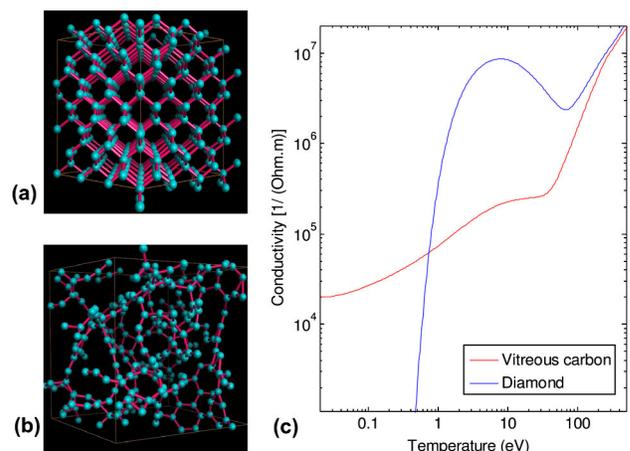

FIG. 2 (color online). Structure of (a) diamond and (b) vitreous carbon. (c) Electrical conductivity as a function of temperature for both carbon allotropes. The curves are calculated as described in the main text.

the electron mean free path in the material [7]. If the ions are highly disordered, then electrons will scatter incoherently and the electron mean free path will be limited to the mean interionic distance, leading to a low conductivity. If, however, the ions are in a well-ordered geometric lattice, then constructive interference of the scattering of the wave function from multiple ions results in a mean free path considerably longer than the mean interionic distance. Thus, for an ordered structure of ions the material conductivity is larger than for a disordered material of the same atomic element, and similar density. At very high temperatures (> 100 eV) the scattering cross sections diminish rapidly with increasing mean electron momentum, typical of Coulomb scattering processes, and hence the conductivity increases irrespectively of ionic ordering.

Next we consider how the calculated differences in electrical conductivity affect the propagation of fast electrons by performing simulations using the 3D ZEPHYROS particle-based hybrid code [12]. A $200 \times 200 \times 200$ μm^3 box with cell size equal to $1 \times 1 \times 1$ μm^3 was used. The laser-to-fast electron conversion efficiency was set to 0.3, the peak laser intensity to 2×10^{20} W cm^{-2}, and the pulse duration to 1 ps. An exponential distribution of electron energies was used with temperature equal to 5.7 MeV (ponderomotive scaling [13]). Example simulation results are shown in Fig. 3, in which 2D slices of the fast electron density in the x-y midplane and the y-z rear plane are plotted. The laser irradiates the targets in the y-z plane at $x = 0$ and the fast electron beam propagates in the x direction. In the simulation of diamond, the fast electron beam is smooth and nonfilamented along its whole length and in its transverse profile at the rear surface. In clear contrast to this, the results of simulations for vitreous carbon show a beam that is filamented along most of its length and exhibits a strongly filamented transverse profile at the rear surface. By carrying out modifications of the simulation parameters we conclude that this result is not a consequence of a particular choice of parameters. A wide range of initial divergence angles gives the same result, as do different choices of the absorption fraction and fast electron temperature scaling. We therefore conclude that these two outcomes reflect a significant qualitative difference between the two materials. The simulations start at a temperature of 1 eV and the conductivity curves converge at >100 eV, and therefore the predicted differences in electron transport result entirely from the differences in conductivity of the two targets in the transient WDM regime.

The sensitivity of the fast electron transport pattern to the target conductivity can be explained in terms of a linear instability analysis of resistive filamentation. The resistive filamentation growth rates were calculated as follows [6]. If we denote

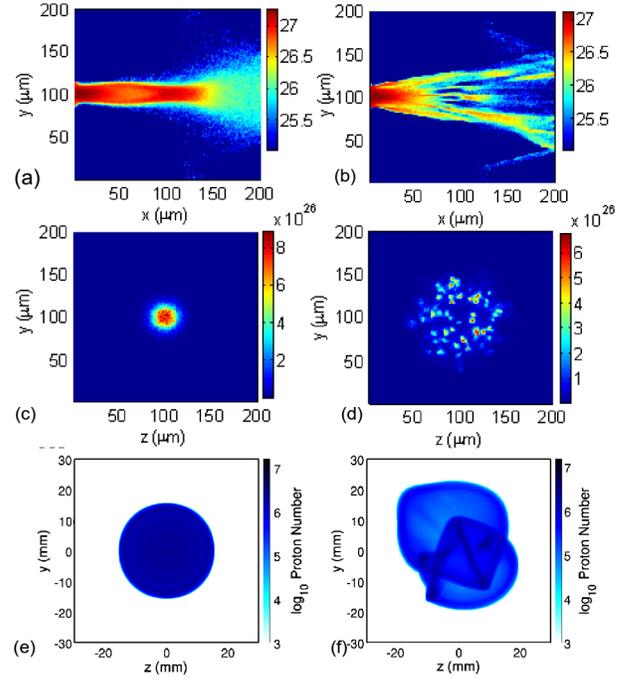$$\alpha = \frac{e^2 u_f^2 n_f^2 \eta k^2}{\gamma m_e} \qquad (1)$$

FIG. 3 (color online).   Fast electron transport simulation results (electron density) for (a),(c) diamond and (b),(d) vitreous carbon; (a) and (b) show the fast electron density distribution within the target (laser incident from left side) at 1.0 ps; (c) and (d) show the same at the rear of the targets after 1.5 ps (when the main part of the current has reached the rear surface). Smooth transport is observed with diamond, compared to heavily filamented transport in vitreous carbon. The calculated spatial-intensity distribution of the resulting proton beam is shown in (e) and (f), respectively.

and

$$\beta = \frac{e T_\perp k^2}{\gamma m_e}, \qquad (2)$$

where u_f, n_f, $T_\perp$, and γ are the fast electron velocity, density, transverse temperature, and Lorentz factor, respectively, η is the resistivity, and k is the wave number of the filamentation mode, then the growth rate of the resistive filamentation mode is

$$\Gamma = (\alpha/2 - \sqrt{D})^{1/3} - (\sqrt{D} - \alpha/2)^{1/3}, \qquad (3)$$

where $D = (\beta/3)^3 + (\alpha/2)^2$. By choosing representative fast electron parameters the resistive filamentation growth rates in the WDM regimes of the two materials (vitreous carbon, $\eta \approx 4 \times 10^{-6}$ Ωm; diamond, $\eta \approx 2 \times 10^{-7}$ Ωm) can be examined. We choose typical values of $n_f = 10^{26}$ m^{-3}, $u_f = c$, $\gamma = 10$ and find that the filamentation growth rate is much larger for vitreous carbon than for diamond. In vitreous carbon, the time for one e-folding of the resistive filamentation instability is on the order of a few tens of femtoseconds. This means that for electron transport driven by a 1 ps laser pulse, strong filamentation should occur—as observed in the hybrid simulations and

experimentally. In diamond the *e*-folding time is at least a few hundred femtoseconds, so the beam is much less likely to filament. Thus the absence of filamentation observed experimentally for diamond compared to other allotropes of carbon results from its much higher conductivity at WDM temperatures, which in turn results due to the highly ordered arrangement of carbon atoms.

Finally, to demonstrate the correlation between the fast electron density distribution at the target rear and the spatial-intensity distribution of the proton beam, an analytical model was developed to compute the evolution of the sheath field, the proton front, and the projection of the protons to the detector plane. The fast electron distributions resulting from the hybrid electron transport simulations [Fig. 3(c) and 3(d)] were used to calculate the electric field distributions. The temporal evolution of the field and the spreading of the electrons on the target surface were modeled using a similar approach to that described by Yuan *et al.* [14]. Field ionization of hydrogen is assumed to produce the protons and their projection to the detector plane is calculated using the local gradients in the proton front. The methodology will be described in detail in a separate publication. Figures 3(e) and 3(f) show the calculated proton beam spatial-intensity distributions corresponding to the fast electron density distributions in Figs. 3(c) and 3(d), respectively. These are in good qualitative agreement with the measurements in Fig. 1.

In summary, these results show, for the first time, that in the interaction of a short high intensity laser pulse with a solid target the effects of lattice structure in defining the electrical conductivity of the induced transient WDM state plays a key role in the transport of fast electrons within the target. This has implications for the many potential applications of high power laser-solid interactions involving the conduction of large currents of energetic electrons. It shows that the choice of allotrope of a given element is important, which impacts on the choice of materials used in the fabrication of advanced targets for fusion (such as the cone, cone wire, and other variant targets proposed for the fast ignition scheme [15]) and in targets for laser-driven ion acceleration. Our finding that diamond produces

smooth electron transport is particularly interesting from an applications viewpoint because of its unique material properties, including high hardness and thermal conductivity.

Furthermore, our analysis shows that the rate of fast electron beam filamentation depends sensitively on electrical conductivity. This suggests that resistive filamentation is the dominant instability mechanism for the parameters explored.

*paul.mckenna@strath.ac.uk
[1] M. Tabak *et al.*, Phys. Plasmas **1**, 1626 (1994).
[2] M. Borghesi *et al.*, Fusion Sci. Technol. **49**, 412 (2006).
[3] E. S. Weibel, Phys. Rev. Lett. **2**, 83 (1959).
[4] Y. Sentoku *et al.*, Phys. Rev. Lett. **90**, 155001 (2003).
[5] B. Hao *et al.*, Phys. Rev. E **79**, 046409 (2009).
[6] L. Gremillet, G. Bonnaud, and F. Amiranoff, Phys. Plasmas **9**, 941 (2002).
[7] J. M. Ziman, Adv. Phys. **16**, 551 (1967).
[8] J. Fuchs *et al.*, Phys. Rev. Lett. **91**, 255002 (2003).
[9] V. Recoules *et al.*, Phys. Rev. Lett. **96**, 055503 (2006).
[10] G. Kresse and J. Hafner, Phys. Rev. B **47**, 558 (1993).
[11] M. P. Desjarlais, J. D. Kress, and L. A. Collins, Phys. Rev. E **66**, 025401 (2002).
[12] S. Kar *et al.*, Phys. Rev. Lett. **102**, 055001 (2009).
[13] S. C. Wilks and W. L. Kruer, IEEE J. Quantum Electron. **33**, 1954 (1997).
[14] X. H. Yuan *et al.*, New J. Phys. **12**, 063018 (2010).
[15] R. Kodama *et al.*, Fusion Sci. Technol. **49**, 316 (2006).